AIP | Applied Physics Letters

Active acoustic metamaterials with tunable effective mass density by gradient magnetic fields

Xing Chen, Xianchen Xu, Shigang Ai, HaoSen Chen, Yongmao Pei, and Xiaoming Zhou

Citation: Applied Physics Letters **105**, 071913 (2014); doi: 10.1063/1.4893921
View online: http://dx.doi.org/10.1063/1.4893921
View Table of Contents: http://scitation.aip.org/content/aip/journal/apl/105/7?ver=pdfcov
Published by the AIP Publishing

Active acoustic metamaterials with tunable effective mass density by gradient magnetic fields

Xing Chen,[1] Xianchen Xu,[2] Shigang Ai,[3] HaoSen Chen,[4] Yongmao Pei,[1,a)] and Xiaoming Zhou[2,a)]

[1]*State Key Lab for Turbulence and Complex Systems, College of Engineering, Peking University, Beijing 100871, China*
[2]*Key Laboratory of Dynamics and Control of Flight Vehicle, Ministry of Education, and School of Aerospace Engineering, Beijing Institute of Technology, Beijing 100081, China*
[3]*Institute of Engineering Mechanics, Beijing Jiaotong University, Beijing 100044, China*
[4]*Department of Engineering Mechanics, Tsinghua University, Beijing 100084, China*

(Received 4 June 2014; accepted 9 August 2014; published online 21 August 2014)

Magnetically controlled acoustic metamaterials are designed and experimentally studied. Magneto-acoustic metamaterials are fabricated by covering an aluminum circular ring with magnetorheological elastomer. The resonant frequency of the structured elastomer is actively tunable by external gradient magnetic field, allowing for values of effective mass density of metamaterials to be adjusted in the low-frequency region. A prestressed plate theory is proposed to explain the shifting of the resonant frequency induced by the magnetic field and coincides very well with the experimental results. It is found that the tunability of magneto-acoustic metamaterials is attributed to the competition between the magnetic-field-induced prestress and the structural flexural rigidity. The proposed magneto-acoustic metamaterials realize the dynamic tuning of effective mass density with non-contact and fast-response gradient magnetic fields, providing a degree of freedom for full control of sound. © *2014 AIP Publishing LLC*. [http://dx.doi.org/10.1063/1.4893921]

Acoustic metamaterials are a kind of artificial material that are capable of implementing some fascinating phenomenon, such as acoustic cloaks,[1,2] focusing and subdiffraction imagining,[3–5] or acoustic diode.[6,7] In order to tailor wave propagation pattern, the focus has been on developing suitable metamaterial structures with designed effective parameters. Recently, membrane-type acoustic metamaterials, consisting of a periodic array of interspaced membranes, were proposed for exhibiting broadband negative effective modulus and density.[8,9] Moreover, membrane-type acoustic metamaterials have been highlighted for unique features in low-frequency noise isolation and absorption.[10–13] The excellent sound attenuation properties of acoustic metamaterial membranes, with an average sound transmission loss of >40 dB, were first noticed by Yang *et al*. over a broad frequency range of 50–1000 Hz.[10] Meanwhile, Mei *et al*. achieved near-unity absorption at the resonant frequency by using thin elastic membranes decorated with designed patterns of rigid platelets.[11]

Despite possessing numerous advantages, passive acoustic metamaterials suffer from the narrow band of operating frequency because of the highly dispersive nature of resonant microstructures. Active acoustic metamaterials, whose properties can be adjusted by external stimuli, have been developed for obtaining a much wider range of effective parameters. Akl and Baz did a lot of pioneering work on developing electric control acoustic metamaterials.[14–18] For instance, they manufactured a 1D fluid domain confined from both ends with PZT4 piezoelectric diaphragms. The voltage applied to the piezoelectric elements through the leads varies its stiffness and via coupling with the fluid domain, the impedance resonance peak shifted from 600 Hz for the uncontrolled case to 450 Hz and 900 Hz for the positive and negative feedback gains, respectively.[14] Besides, various active cells were proposed for realizing programmable dynamic density or bulk modulus.[15–18] Popa *et al*. demonstrated an electrically actuated acoustic metamaterials whose effective density and effective modulus can be tuned independently.[19] However, the contact control lacks of stability and feasibility under some complex environment. Thus, it is significant to study non-contact tuning methods to overcome these limitations.

In this paper, attempts have been carried out to develop a non-contact tuning approach availably for magnetic membrane-type acoustic metamaterials. The impedance tube is adopted to investigate its acoustical properties in magnetic fields. The mechanism of tuning negative effective mass density, due to the magnetic-induced prestress improving structural stiffness, is revealed. In addition, there exists a competitive relation between the prestress and the flexural rigidity of the structure for determining the resonance characteristics. A prestressed plate theory is proposed to illustrate magnetic field induced frequency shift and is in good agreement with the experimental results.

The membrane structure comprises an elastic membrane and a support frame as shown in Fig. 1(a). The support frame is a pair of circular aluminum rings with an outer diameter of 29 mm and a thickness of 10 mm designed to fit snugly in the testing apparatus. The elastic membrane, with a radius a of 9 mm and thickness t of 0.5 mm, is fixed by the support frame. The photo of the sample is also shown in Fig. 1(b). The elastic membrane is fabricated with magnetorheological elastomers which are a kind of magnetic field-responsive smart polymer composites. The magnetorheological

a)Authors to whom correspondence should be addressed. Electronic addresses: peiym@pku.edu.cn (Tel.: +86-10-62757417) and zhxming@bit.edu.cn

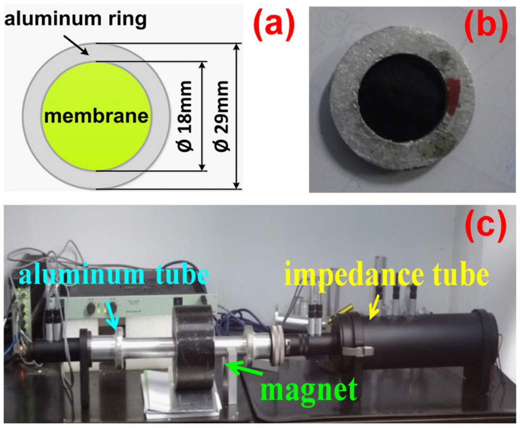

FIG. 1. (a) The schematic of the membrane structure. (b) The front view of the membrane structure. (c) The experimental measurement device.

elastomers used in this study consist of nearly spherical Fe_3O_4 particles embedded in silicone rubber. The particle sizes range from approximately 10 μm to 100 μm and have a mass fraction of 60%. With the aid of the necessary cross-linkers and processing materials, these materials are mixed together on a typical two-roll mill. After all ingredients are evenly mixed in a mixing machine, the mixture is packed in a mold and then cured with a temperature of roughly 333 K for approximately 2 h. Young's modulus E, density ρ and Poisson's ratio ν for the membrane material is 6.9 MPa, 2100 kg/m^3, and 0.45, respectively. The structure is placed in the middle of the non-magnetic aluminum tube and the transmission loss TL of the sample is measured in the impedance tube as shown in Fig. 1(c).

The acoustical properties of the membrane structure are investigated in gradient magnetic fields. A hollow cylindrical magnet, with axial length of 100 mm and inner diameter of 52 mm, is used to generate a magnetic field. The magnetic field can be decomposed into a uniform radial magnetic field and a gradient axial magnetic field. The axial magnetic field is measured by Gauss Meter as the distance X between the center of the magnet and test point varies. It can be seen from the Fig. 2(a) that the axial magnetic field gradient increases as the location closes to the edge of the magnet. The maximum gradient magnitude is obtained at $X = \pm 50$ mm, while the magnetic field can be regarded as uniform around $X = 0$ mm. The magnetic field can be varied by adjusting the relative location between the magnet and the sample. We test the sample in every 10 mm increment of the relative location. The measured transmission loss and effective mass density over a frequency range of 100–1000 Hz are shown in Figs. 2(b) and 2(c), respectively. The effective mass density can be calculated by dividing the averaged stress by the averaged acceleration over the whole membrane, i.e., $\rho_{eff} = \langle \sigma_{xx} \rangle / \langle a_x \rangle$, while the stress σ_{xx} and acceleration a_x normal to the membrane plane can be derived from the measured transfer matrix. It is observed that the membrane structure exhibits negative effective mass density below the first order resonant frequency. Physically, negative effective mass density origins from the out-of-phase average acceleration with the pressure gradient. In the vicinity of the resonant frequency, unbounded average acceleration leads to zero density. What is more, negative effective mass density, along with the resonance frequencies, can be tuned by gradient magnetic field. As the magnetic field gradient increases, negative effective mass density expands to a wider range and the resonant frequencies shift to a higher level. Thus, the mechanism of tuning negative effective mass density can be understood through the resonance characteristics of acoustic metamaterials. When the magnetic field gradient reaches the maximum at $X = 50$ mm, the first order resonant frequency of the membrane structure, referring to the absence of the magnetic field, can be improved by 64%. However, the increment of the second order resonant frequency is only 15%. It implies that the gradient field plays a dominant role in lower frequency.

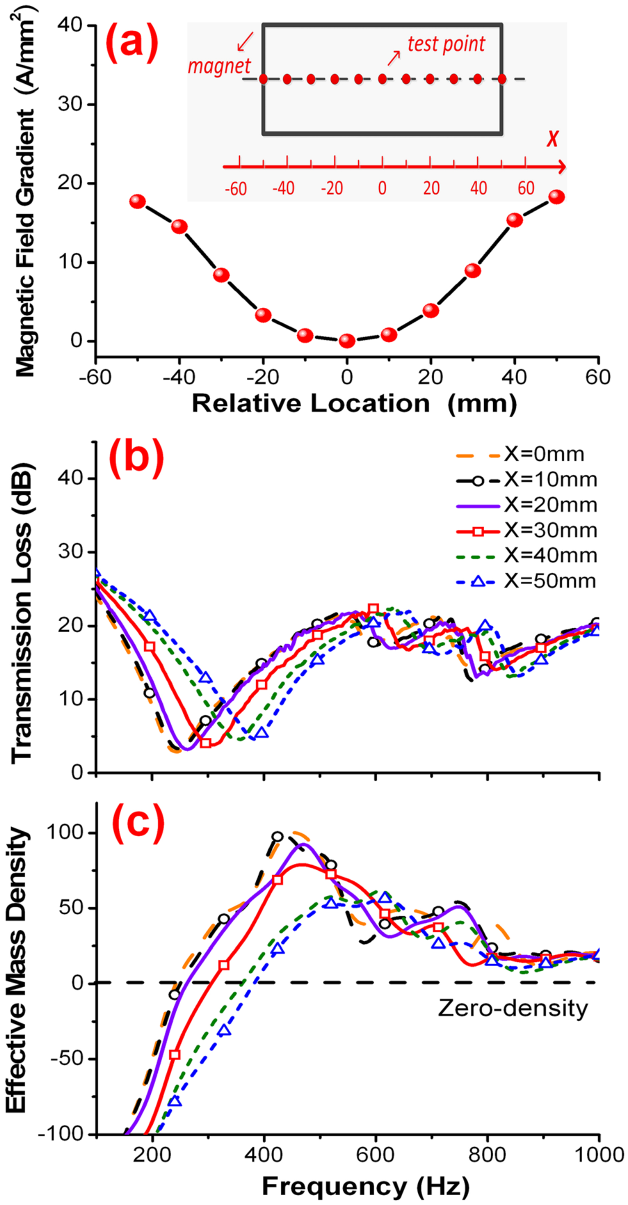

FIG. 2. (a) The magnetic field gradient varies along the axial direction. Inset: The schematic of test points. (b) The measured STL spectra in different gradient magnetic fields. (c) The effective mass density in different gradient magnetic fields.

The acoustical properties of the membrane structure are also investigated in uniform magnetic field of 430 KA/m and without magnetic field, respectively. The measured transmission loss of the membrane structure is shown in Fig. 3. Two transmission loss dips at 236 Hz and 748 Hz, and two peaks at

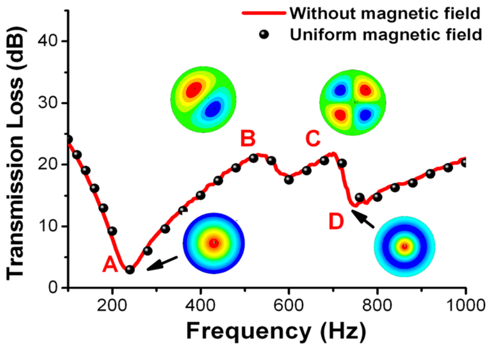

FIG. 3. The measured transmission loss curve of the membrane structure. Inset: The vibration mode shapes of the membrane structure at the characteristic frequencies (a) first axisymmetric resonant frequency (b) first nonaxisymmetry resonant frequency (c) second nonaxisymmetry resonant frequency (d) second axisymmetric resonant frequency.

449 Hz and 702 Hz, are clearly seen. The transmission loss spectrum shows that the near-total reflection occurs around the transmission loss peaks. For a better understanding of these transmission properties, we conduct a modal analysis with finite element method. There are four eigenmodes in the considered frequency range as shown in the inset of Fig. 3. The points A and D in the transmission loss dips correspond to the first and second axisymmetric resonances, respectively, while the anti-resonant frequency relate to the points B and C in the transmission loss peaks. When the excitation frequency of sound source is close to the structural axisymmetric resonant frequency, the near-zero effective mass contributes to total transmission.[13] In the vicinity of the anti-resonant frequency, the averaged out-of-plane displacement is nearly zero. The cell thus acts like a nodal point on average in wave propagation and the transmission thereby reaches a minimum. This behavior is consistent with the results reported in Ref. 20. Furthermore, magnetorheological elastomers are known as the overall shape and elastic properties can be altered rapidly and reversibly by an applied uniform magnetic field.[21,22] The mechanism responsible for this bulk effect is the induced magnetic interaction between the ferromagnetic particles in the composite.[23] However, it can be seen from Fig. 3 that the acoustical properties of the magnetic film are insensitive to the uniform magnetic field. It implies that the influence of the uniform magnetic field on the mechanical properties can be ignored in this case. In comparison with the situation in gradient magnetic fields, it indicates that the force, induced by the gradient magnetic field, is highlighted for tuning effective mass density.

Comparing the experimental results in different kinds of magnetic fields, we conclude that the prestretching induced by magnetic force is responsible for tuning effective mass density. For a better understanding of the tuning mechanism, a prestressed plate theory is proposed to illustrate how the magnetic field affects the resonance characteristics of magnetic membrane. In consideration of $h/R > 1/80$, the membrane is treated as a plate for this case. The governing equations of the membrane, taking into account the prestress effect, can be expressed as:

$$D\nabla^4 w - Th\nabla^2 w + \rho h \frac{\partial^2 w}{\partial t^2} = P, \qquad (1)$$

where w is the out-plane displacement; D is the flexural rigidity of the plate; T, acting as prestress, is the tension per unit length; P is the applied load along the normal direction. The vibration is assumed as harmonic, and the trial solution is written as $w(r,\theta,t) = \eta_a(r,\theta)\, e^{j\omega t}$ in polar coordinates. The vibration mode function is derived from separation variable method:

$$\eta_{am}(r,\theta) = (A_m J_m(k_1 r) + B_m I_m(k_2 r))e^{jm\theta}, \qquad (2)$$

where $k_{1,2} = \left(\frac{\sqrt{T^2+4D\rho h\omega^2}\mp T}{2D}\right)^{1/2}$ are parameters in determining the characteristic frequencies; the constants A_m and B_m are derived from the initial condition; J_m and I_m are mth Bessel function of the first kind and modified mth Bessel function of the first kind, respectively. For axisymmetric vibration, m is equivalent to zero. Substituting the boundary conditions of the clamped plate into Eq. (2), the resonant frequency is calculated by:

$$\begin{vmatrix} J_m(k_1 a) & I_m(k_2 a) \\ \left(\dfrac{d\,J_m(k_1 r)}{dr}\right)_{r=a} & \left(\dfrac{d\,I_m(k_2 r)}{dr}\right)_{r=a} \end{vmatrix} = 0. \qquad (3)$$

From the expression of $k_i (i = 1,2)$, it implies that the prestress T competes with the structure parameters in determining structural vibration properties. It is especially highlighted for the flexible membrane structure because of its low the flexural rigidity. The prestress is the main factor contributing to the structural stiffness in low frequency, while the influence of the prestress can be ignored in high frequency range.

The source of the tension T can be decomposed into prestretching prestress T_1 and magnetic-induced prestress T_2. When the direction of magnetic field gradient is perpendicular to the membrane, normal surface traction is uniformly applied. The magnetic force is:[24]

$$P_0 = h\,\mu_0 M \nabla H, \qquad (4)$$

where μ_0 is the vacuum permeability, H is the magnetic field intensity, M is the magnetization of the magnetorheological elastomer. We assume that the membrane would deform into a spherical cap, and the strain and the stress is uniform through the film following Hooke's law. The strain is defined as the change in arclength divided by the original arclength. The strain and the stress are derived from geometrical considerations and the condition of force equilibrium, respectively. When the film deflection w is much less than its radius a, the strain and the stress are calculated with the following result:

$$\varepsilon = \frac{2w^2}{3a^2} \quad \text{and} \quad \sigma = \frac{P_0 a^2}{4hw}. \qquad (5)$$

Combining the constitutive relation with Eq. (5), the magnetic-induced prestress T_2 is expressed as:

$$T_2 = \left[\frac{Eha^2 P_0^2}{24(1-\nu)}\right]^{\frac{1}{3}}. \qquad (6)$$

It can be seen from Eq. (6) that the magnetic-induced prestress increases with the magnetic field gradient. The axisymmetric

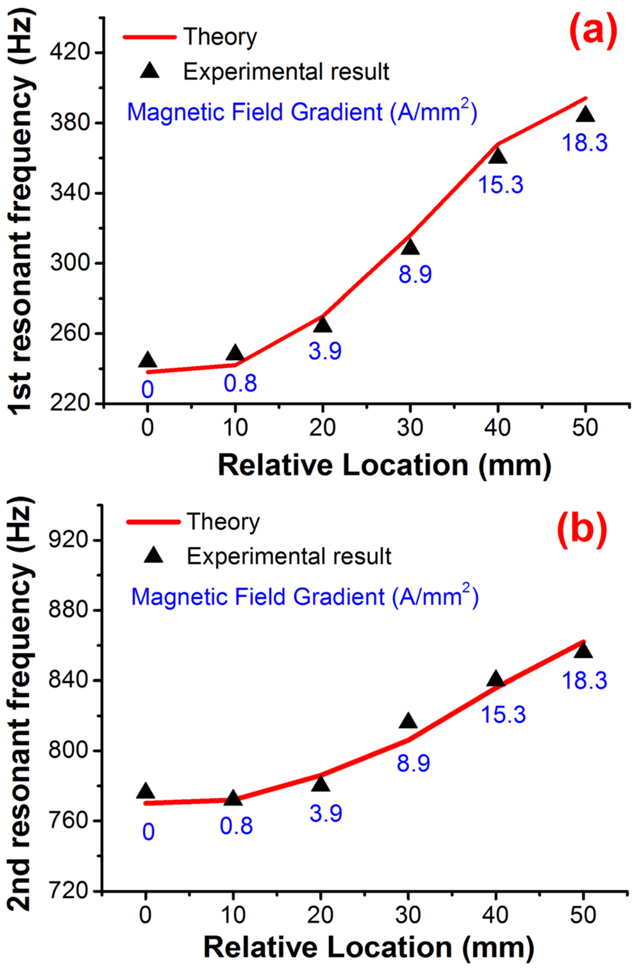

FIG. 4. (a) The theoretical prediction of 1st resonant frequency and the experimental result in different gradient magnetic field. (b) The theoretical prediction of 2nd resonant frequency and the experimental result in different gradient magnetic field.

resonant frequencies in different gradient magnetic field are calculated from Eq. (3). The theoretical prediction has good agreement with the experimental result as shown in Fig. 4. In order to reveal the intrinsic reason for tunable frequency, the magnetic field gradient is marked at the test points. The prediction of the first order resonant frequency is shifted from 238 to 394 Hz as the magnetic field gradient increases. It can be known from the expression of k_i that the prestress is the main factor contributing to the structural stiffness in low frequency. Thus, the first order resonant frequency, derived from the vibration of the membrane approximately, can be calculated by $f_1 = \frac{2.405}{2\pi a}\sqrt{\frac{T}{\rho h}}$. Combing with Eq. (6), it shows that the increment of the first order resonant frequency slows down as the magnetic field gradient increases. Besides, it also can be seen from the expression of k_i that the structural flexural rigidity plays an important role in determining the vibration properties in high frequency range. The competitive relation between the prestress and the structural flexural rigidity leads to the weaker resonant frequency shift phenomenon in high frequency as the theoretical predictions.

In summary, the acoustical properties of membrane-type acoustic metamaterials in magnetic fields are investigated. Tunable effective mass density by gradient magnetic fields is reported. The tuning mechanism is attributed to magnetic-induced prestress improving structural stiffness, which is understood by analysis of the resonance characteristics. Besides, a prestressed plate theory is developed to illustrate this phenomenon and shows good agreements with the experimental results. It implies that there exists a competitive relation between the prestress and the flexural rigidity of the structure for determining the resonant frequency. The magnetic-induced prestress is highlighted for its tuning effect in low frequency. A non-contact tuning method, triggering by gradient magnetic field, is proposed for membrane-type acoustic metamaterials which paves a way for having a full control of wave propagation.

Supported by the National Natural Science Foundation of China (11090330, 11090331, 11202007, 11221202, and 11072003) and the Chinese National Programs for Scientific Instruments Research and Development (2012YQ03007502). Support by the National Basic Research Program of China (G2010CB832701) is also acknowledged. Program for New Century Excellent Talents in University (Grant No. NCET-11-0794).

[1]M. Farhat, S. Guenneau, and S. Enoch, Phys. Rev. Lett. **103**, 024301 (2009).
[2]B. I. Popa, L. Zigoneanu, and S. A. Cummer, Phys. Rev. Lett. **106**, 253901 (2011).
[3]J. Li, L. Fok, X. Yin, G. Bartal, and X. Zhang, Nature Mater. **8**, 931 (2009).
[4]J. Zhu, J. Christensen, J. Jung, L. Martin-Moreno, X. Yin, L. Fok, X. Zhang, and F. Garcia-Vidal, Nat. Phys. **7**, 52 (2011).
[5]X. Zhou and G. Hu, Appl. Phys. Lett. **98**, 263510 (2011).
[6]B. Liang, B. Yuan, and J. C. Cheng, Phys. Rev. Lett. **103**, 104301 (2009).
[7]B. Liang, X. S. Guo, J. Tu, D. Zhang, and J. C. Cheng, Nature Mater. **9**, 989 (2010).
[8]S. H. Lee, C. M. Park, Y. M. Seo, Z. G. Wang, and C. K. Kim, Phys. Rev. Lett. **104**, 054301 (2010).
[9]M. Yang, G. Ma, Z. Yang, W. Wen, and P. Sheng, Phys. Rev. Lett. **110**, 134301 (2013).
[10]Z. Yang, H. M. Dai, N. H. Chan, G. C. Ma, and P. Sheng, Appl. Phys. Lett. **96**, 041906 (2010).
[11]J. Mei, G. Ma, M. Yang, Z. Yang, W. Wen, and P. Sheng, Nat. Commun. **3**, 756 (2012).
[12]C. J. Naify, C. M. Chang, G. McKnight, F. Scheulen, and S. Nutt, J. Appl. Phys. **109**, 104902 (2011).
[13]Y. Zhang, J. Wen, H. Zhao, D. Yu, L. Cai, and X. Wen, J. Appl. Phys. **114**, 063515 (2013).
[14]W. Akl and A. Baz, J. Appl. Phys. **111**, 044505 (2012).
[15]A. Baz, New J. Phys. **11**, 123010 (2009).
[16]W. Akl and A. Baz, J. Intell. Mater. Syst. Struct. **21**, 541–556 (2010).
[17]W. Akl and A. Baz, Smart Mater. Struct. **20**, 125010 (2011).
[18]W. Akl, A. Elsabbagh, and A. Baz, J. Acoust. Soc. Am. **132**, 2857 (2012).
[19]B. I. Popa, L. Zigoneanu, and S. A. Cummer, Phys. Rev. B **88**, 024303 (2013).
[20]Z. Yang, J. Mei, M. Yang, N. H. Chan, and P. Sheng, Phys. Rev. Lett. **101**, 204301 (2008).
[21]R. V. Ramanujan and L. L. Lao, Smart Mater. Struct. **15**, 952 (2006).
[22]X. Zhao, J. Kim, C. A. Cezar, N. Huebsch, K. Lee, K. Bouhadir, and D. J. Mooney, Proc. Natl. Acad. Sci. **108**, 67 (2011).
[23]L. Borcea and O. Bruno, J. Mech. Phys. Solids **49**, 2877 (2001).
[24]L. E. Faidley, Y. Han, K. Tucker, S. Timmons, and W. Hong, Smart Mater. Struct. **19**, 075001 (2010).